Data driven modeling and estimation of accumulated damage in mining vehicles using on-board sensors

Erik Jakobsson[1,2], Erik Frisk[2], Robert Pettersson[1], and Mattias Krysander[2]

[1] *Atlas Copco Rock Drills AB, Örebro, 702 25, Sweden*
erik.jakobsson@se.atlascopco.com
robert.pettersson@se.atlascopco.com

[2] *Linköping University, Linköping, 581 83, Sweden*
erik.frisk@liu.se
mattias.krysander@liu.se

Abstract

The life and condition of a MT65 mine truck frame is to a large extent related to how the machine is used. Damage from different stress cycles in the frame are accumulated over time, and measurements throughout the life of the machine are needed to monitor the condition. This results in high demands on the durability of sensors used. To make a monitoring system cheap and robust enough for a mining application, a small number of robust sensors are preferred rather than a multitude of local sensors such as strain gauges. The main question to be answered is whether a low number of robust on-board sensors can give the required information to recreate stress signals at various locations of the frame. Also the choice of sensors among many different locations and kinds are considered. A final question is whether the data could also be used to estimate road condition. By using accelerometer, gyroscope and strain gauge data from field tests of an Atlas Copco MT65 mine truck, coherence and Lasso-regression were evaluated as means to select which signals to use. ARX-models for stress estimation were created using the same data. By simulating stress signals using the models, rain flow counting and damage accumulation calculations were performed. The results showed that a low number of on-board sensors like accelerometers and gyroscopes could give enough information to recreate some of the stress signals measured. Together with a linear model, the estimated stress was accurate enough to evaluate the accumulated fatigue damage in a mining truck. The accumulated damage was also used to estimate the condition of the road on which the truck was traveling. To make a useful road monitoring system some more work is required, in particular regarding how vehicle speed influences damage accumulation.

Figure 1. The mine truck model on which the study was performed.

1. Introduction

The life and condition of a mining vehicle is to a large extent related to how the machine is used. A machine carrying heavy loads and driving fast in rough terrain, deteriorates faster than a lightly loaded machine creeping along paved roads. Methods exist to evaluate the fatigue damage of a structure, given a measurement of the strain or stress in the structure. Such measurements typically require strain gauge sensors, which are too fragile and expensive to be used for any longer period in a live application.

To make a useful system economically feasible to roll out on a large number of machines, one would need to use cheaper and more robust types of sensors, still capable of estimating the stresses and strains that the machine experiences. Ideally this would be sensors already available on the machines today. This paper focuses on using accelerometers and gyroscopes as the main sensors to estimate the stress and fatigue in the mine truck frame. These sensors are currently not available as standard on Atlas Copco machines, but they could be on future products.

One way to create such a system for a ground vehicle is to identify and categorize the type of terrain (Heine & Barker, 2007). The method includes determining the rate of damage accumulation for a number of predefined terrain types at known test tracks. Statistics such as mean and kurtosis from accelerometer data are then used to identify the current terrain type, damage is summed up, and thus a measure of accumulated damage is calculated. The simplicity of this approach is appealing, but to characterize mine roads into different types is problematic, since they can cover they full scale from flat to very rough.The method is likely too coarse for this application.

Another method (Rupp, Masieri, & Dornbusch, 2005) estimates accumulated damage directly from accelerometer signals. Their approach involves extracting acceleration data in different frequency bands, and to estimate the damage increment for each acceleration signal. This generates 15 different damage increment measures. Artificial neural networks are used to find how to combine the different damage increments into actual accumulated damage as measured by strain sensors. No recreation of the actual strain signals is performed, and thus it can be difficult to have a full physical understanding from acceleration to accumulated damage.

This work intends to overcome previous limitations by creating a model for damage accumulation without the need for predefined terrain types. The model should also maintain the physical connection between stress and accumulated damage. That is, the estimated accumulated damage should correspond to the real accumulated damage, and both should derive from the same peeks and valleys of the stress signal. The stress signals can be interpreted and verified against measured data which is believed important since it is often difficult to obtain verification data for actual failures of machines.

To combine accelerometer, gyroscope and other sensor data to recreate a stress signal requires a model, and if this model is to be run in real time on-board a vehicle, considerations must be made due to the limited computational resources available. Running for example a Finite Element Model consisting of the entire vehicle is impossible given those constraints. This work therefore targets to use significantly simpler, linear dynamic models.

The study was conducted with data from a prototype version of the Atlas Copco MT65 mine truck in both highly monitored test-track driving, and from operational mine sites.

2. PROBLEM FORMULATION

The main question to be answered is whether a low number of robust on-board sensors can give the required information

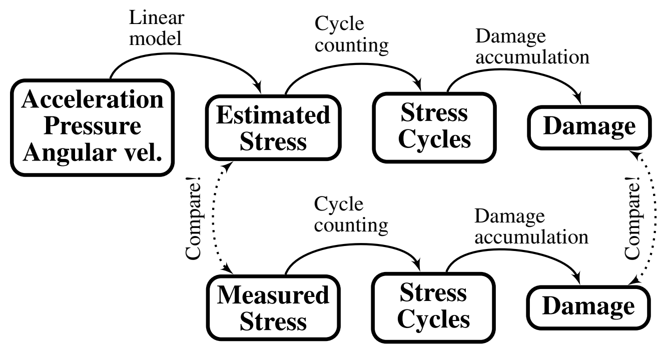

Figure 2. Schematic view of the process for calculating accumulated damage and comparing the results.

to recreate stress signals at various locations of the frame. Since several different sensor types and positions are possible, a first problem is to find methods for evaluating what input signals to use for a given output signal. Only the sensor locations available in the data set are considered in this paper.

The recreated stress signals needs to be accurate enough to capture the peaks and valleys of the measured signal in order to perform fatigue damage analysis. A second problem is whether a simple linear model is sufficient to reach such accuracy, and what order of model complexity is required. The models are evaluated by comparing the accumulated damage of the recreated and measured stress signals respectively, but also by comparing stress directly. A schematic view of the process is illustrated in Figure 2.

One factor believed to be important for the damage accumulation is the condition of the road on which the machine is traveling. A third problem is therefore to investigate if the recreated stress signals also can be used to determine road condition.

The on-board sensors considered are limited to accelerometers, gyroscopes, speed and pressure sensors. The output signals considered are the strain gauges available in the data set, since the measurements were already completed when this work started.

A number of use-cases exists for the truck, and they all contribute to damage accumulation in the structure. The main focus of this paper is a driving case, which includes both driving with loaded, and driving with an empty dump box.

3. RAIN FLOW COUNT AND ACCUMULATED DAMAGE

Cycle counting and damage accumulation was used to evaluate the damage caused by a certain stress-time signal. A typical metallic material can withstand a certain number of load cycles with a given stress range before failure. The number of cycles are dependent on the cycle amplitude, and the relation is often presented in the stress to number of cycles-diagram or SN-diagram for short. More information on metal

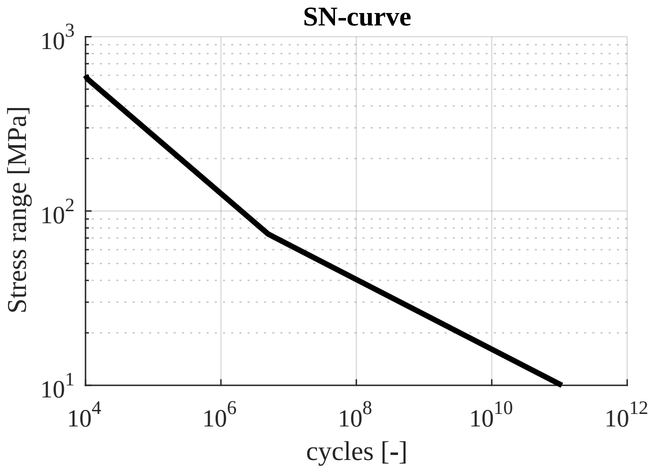

Figure 3. Relationship between stress range and the number of cycles until fatigue failure occurs for a given probability, here 2.3%. For a given stress range level, the structure can withstand a number of cycles as given by the curve.

fatigue and SN-diagrams can be found in (Stephens, Fatemi, Stephens, & Fuchs, 2000). For this work, the SN-diagram (Byggavdelningen, Göransson, & Åkerlund, 1999) in Figure 3 was used.

A recognized way to handle spectral time-stress signal containing many different stress amplitudes is by using the rain flow counting method (ASTM E 1049-85 (Reapproved 1997), 1999) and then to apply the Palmgren-Miner rule for damage accumulation (Palmgren, 1924). Rain flow counting is used to define load cycles of varying amplitude from a stress-time-signal. The cycles are sorted in bins according to stress amplitude, and the Palmgen-Miner rule stated as

$$D = \sum_{i=1}^{k} \frac{n_i}{N_i} \tag{1}$$

is used to evaluate and sum up the accumulated damage for each bin. In Equation 1, n_i is the number of cycles at the stress amplitude indexed by i from the rain flow count, and N_i is the number of constant amplitude cycles until fatigue failure at the same stress range given by the SN-diagram. The accumulated damage D is defined so that $D = 1$ means a 2.3% failure rate. This corresponds to 2 standard deviations less than 50% failure rate.

4. SYSTEM AND DATA

To give the reader some more background on the techniques used and the data available, a short summary follows. This section also contains some more details on the application in which the study was performed, and what sensors were used.

4.1. System description

The MT65 mine truck is a heavy-duty machine designed for usage in underground mining. Equipped with a 567 kW engine, it is rated for 65 metric tons payload. A typical usage cycle includes the following:

- Loading, when a wheel loader drops rock material into the dump box of the truck. Typically 3 scoops are required to fill the dump box, resulting in over 20 metric tons per scoop.
- Hauling, when the truck moves the material. A common scenario is driving up a steep incline, possibly for hours, until the machine reaches the surface of the mine. Roads vary from paved roads to very rough gravel roads.
- Dumping, when the truck lifts the dump box and the load is tipped off.
- Driving empty, when the truck drives back to be filled once more.

There is also a risk other use cases contribute with a non-negligible amount to the accumulated damage of the machine. Examples of such cases are compaction of the load using a large wheel-loader or hitting the rock wall while driving.

4.2. Available on-board sensors

The machines used for the study contained a number of high sampling rate sensors not commonly available on the Atlas Copco Mine trucks. Some sensors included multiple directions, which is indicated with x,y,z in the sensor name. Most sensors are shown in Figure 4.

The candidates for input signals were:

- Two 3-axis accelerometers, (a1 and a2)
- One 2-axis accelerometer, (a3)
- Two pressure sensors for steering cylinders, (p1 and p2)
- Two pressure sensors for damping cylinders, (p3 and p4)
- One 3-axis gyroscope, (g1, only on a few experiments)
- Vehicle speed, (e1)

The candidates for output signals were:

- 25 strain gauges attached to the frame and dump box of the machine, s1-s25

For a shorter measurement period it is possible to use strain gauges, even if they are considered too fragile to be useful during the full life of a machine. A few of the measurements also contained a GPS tracker, enabling investigation of location dependency and road condition.

4.3. Measurement data

Two sets of data were available for the study. One set from experiments on an internal test track, and one set from normal production at an operational mining site. Data from the

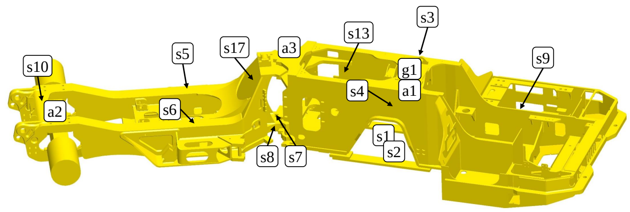

Figure 4. A selection of sensor locations on the mine truck frame. Remaining sensors s18-s25 where located on the dump box, not included in this image.

Table 1. Description of Driving cases

Name	Description	Load [t]	Duration [s]
lc1-1	Defined obstacles	57	2:08
lc1-2	Defined obstacles	57	3:11
lc2-1	Test track,	0	27:58
lc2-2	Test track,	0	21:57
lc3-1	Test track,	57	23:32
lc3-2	Test track,	57	18:54
lc4-1	Test track, low speed	70	22:10
lc5-1	Test track, high speed	70	24:31
lc6-1	Test track, high speed	0	23:45
lc7	Mine site	varying	

customer site covers many months of driving, loading and unloading. It is however not known exactly what has affected the machine at all times in this data set. Data was sampled at 500Hz for this set.

Data from the internal test track was collected during well-defined experiments. This gave the added value of knowing exactly how the machine was operated, and on what type of road. Most experiments were duplicated, giving the possibility to use one part of the data for estimation, and the other for verification. Data was sampled at 2000Hz for this set. Some of the available experiments can be seen in Table 1.

The measurement data was processed in order to simplify the analysis. Since the outcome of interest is rain flow counting, the amplitude of the stress ranges are more important than the absolute level of stress. The accelerometers used had a bandwidth between 0.5Hz to 5kHz, and thus frequencies below 0.5Hz could not be accurately modeled. Signal mean levels were therefore removed from both input and output signals.

The strain gauges were placed in locations where the stress gradient is low, to minimize the effect of small errors in position of the sensors. As a result, a transfer function is required to translate the measured stress to stress in an actual critical point. Throughout this work, a constant amplification of 3.0 was assumed. If a more accurate value is required, it can be found via FEM analysis, but this was deemed unnecessary for the comparative nature of this work.

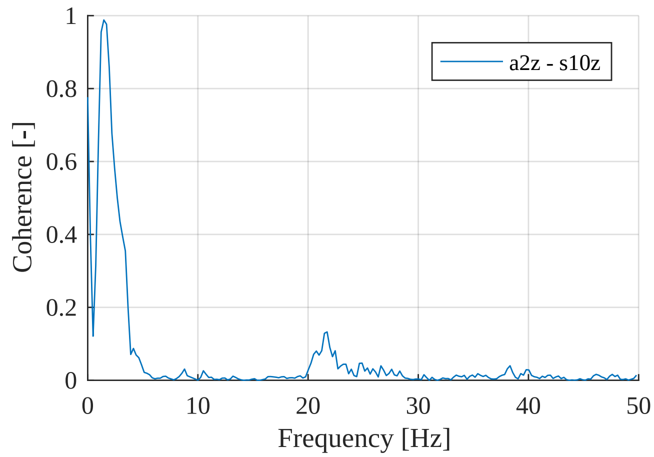

Figure 5. Coherence over the entire frequency range between signal a2z and s10z. Between 0-4Hz coherence is high, indicating a linear relationship between the signals.

5. SELECTION OF SIGNALS

In order to minimize the complexity of a future measurement system, it is important to have as few sensors as possible. To reduce the number of input signals, work was done to investigate what input signals contained the most information to describe a given output signal. In this section two methods for comparing the input signals are investigated. Coherence is often used in the field of modal analysis, and the Lasso originates from statistical analysis and system identification.

To some extent, the techniques were also used to select what output signals to use, i.e., which strain signals would be possible to estimate with the available input signals in the data set.

5.1. Coherence

The magnitude squared coherence C_{yx} is defined as

$$C_{yx}(f) = \frac{|G_{yx}(f)|^2}{G_{xx}(f)G_{yy}(f)}, \tag{2}$$

where $G_{yx}(f)$ is the cross spectral density, and $G_{xx}(f)$, $G_{yy}(f)$ the auto-spectral density for the input- and output signal respectively.

Coherence gives information on how well a linear relation describes the input-output power relationship, for each frequency. A low coherence indicates either a lack of relation between input and output, or that the relation is non-linear.

Typical coherence for a specific input-output combination can be seen in Figure 5. It is clear the main linear relation between input-output exists in the lower frequency region. For higher frequencies coherence is low, indicating a lack of linear relation. There might still exist non-linear relations, but coherence carry no information whether that is the case.

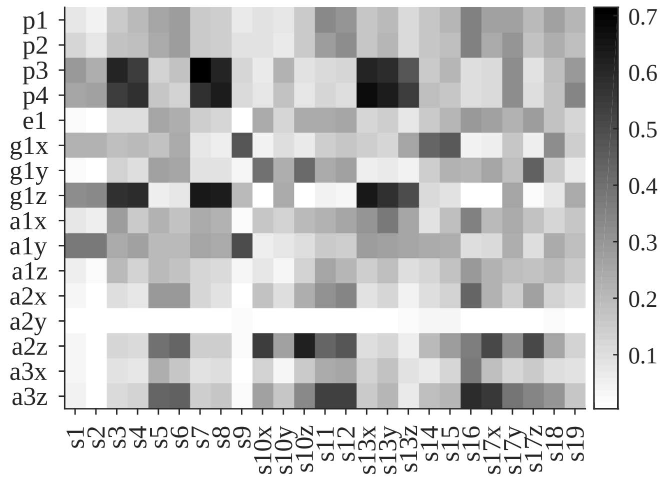

Figure 6. The shade of each square indicates the average coherence in the range 0-3Hz between two signals. The vertical axis contains input signals, and the horizontal axis output signals. A bright row thus indicates an input signal with low coherence to most output signals, i.e. not a very useful signal, and a dark row vice versa. A dark column indicates an output signal with many options for choosing what input signal(s) to choose for modeling it, and a bright column vice versa.

To get an overview of what signal combinations showed linear relations, a measure of average coherence was created. Each coherence plot was reduced to a single value by averaging over parts of the frequency interval. By investigating the frequency content of the output signals, it was found that signal energy is reduced by approximately 10dB/decade after 3Hz. Due to low energy in higher frequencies, an average coherence in the range 0-3Hz was chosen to find what input signals are the best candidates for modeling the output signals. Damage accumulation was also seen to occur mainly due to low frequency oscillations. Figure 6 shows an overview of the average coherence for the input/output combinations.

5.2. Lasso regression

An alternative method used to evaluate the descriptive power of the different input signals is the Lasso (Tibshirani, 1996).

$$\min_{\theta} \left\{ \frac{1}{2N} \|Y - \varphi\theta\|^2 + \lambda \sum_i |\theta_i| \right\} \tag{3}$$

Where φ is a matrix where each row is an observation vector consisting of previous values. Y is the output vector, θ is the parameter vector containing all parameters to be estimated and λ the complexity parameter or penalizing factor. The length of the parameter vector, i.e., the number of time steps used for each input signal, was chosen to 40 time steps, corresponding to 0.2s. Optimization problem 3 is solved for a large number of λ, using the "Glmnet for Matlab" (Qian, Hastie, Friedman, Tibshirani, & Simon, 2013) software package.

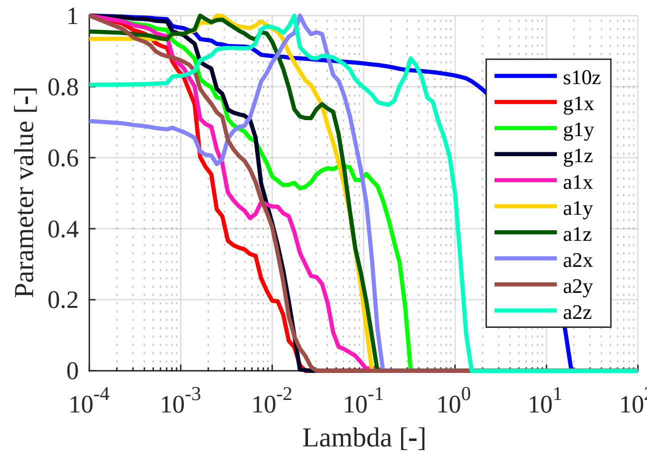

(a) Parameters approach and reach zero as the penalizing factor λ is increased. Each line represent the maximum of all parameters related to the specific input signal.

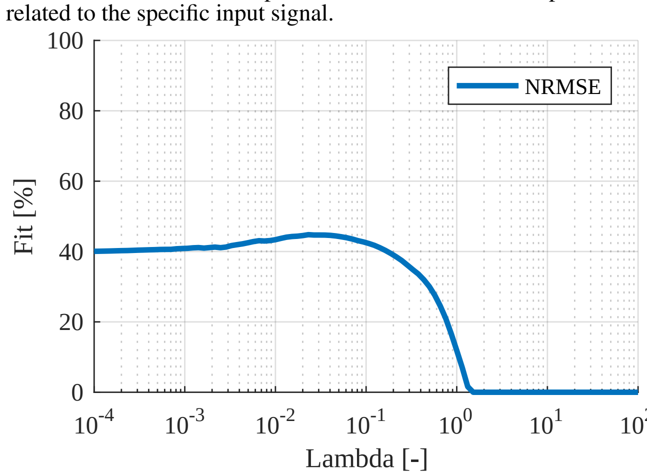

(b) Goodness of fit-measure for increasing lambda.

Figure 7. Input signal selection for $s10z$ by using lasso regression. At $\lambda \approx 0.05$, NRMSE fit is high, and the corresponding signals found in (a) can be chosen. Including more signals over-fits the estimation data, and the NRMSE fit is reduced for the verification data.

Shown in Figure 7a, higher λ punishes the existence of parameters harder, causing one parameter after another to reach zero as λ increases. Figure 7b shows a goodness-of-fit measure, normalized root mean square error or NRMSE, created from validating against a verification data set. NRMSE is defined as

$$NRMSE = 100 \left(1 - \frac{\|y - \hat{y}\|}{\|y - mean(y)\|} \right), \tag{4}$$

where y is the verification data output and $\hat{y}$ the model output.

Ideally a peek is seen in the goodness measure, hinting what λ gives the best fit. For output signal s10z, a maximum is present at $\lambda \approx 2 \cdot 10^{-2}$, using 6 different input signals according to Figure 7a.

The Lasso can also be used to reduce the order of the ARX model, since the lasso technique shows not only the full input signals contribution, but also the contribution of each individual time step for each input signal. For clarity the individual parameters are not included in Figure 7a.

5.3. Results from signal selection

The selected signals from coherence are presented in Table 2. Both the coherence and the Lasso regression method showed similar results on ranking the importance of the input signals. The preferred method to get an overview was the coherence method, since it required no initial assumption on number of parameters. It does however require some initial investigation on what frequency range is of interest to recreate the stress signal.

The Lasso method required assumptions on how many time steps to include in the model estimation. Finding this number is typically an iterative process. Combined with the cross-validation using NRMSE on a verification data set, the Lasso gave a good estimation on what model accuracy to expect from different input signal choices.

For an output signal overview, coherence is the method of choice, since it can be used to present multiple signal combinations at once. To select what output signals are possible to model, one merely needs to see if any input signal shows coherence in the frequency region of interest. For a metric on how accurate the model will be, the Lasso method can be used since it involves a direct measure of the modelling error.

Using the information in Figure 6, the best accelerometer coherence was found for signal $s10z$, which is a stress component at the rear of the truck. Since the accelerometers were available in all experiments of the data set, $s10z$ was chosen to be investigated further. Focusing on $s10z$, the best candidates for input signals where $g1y$ and $a2z$, as given by Figure 6. Figure 7a show that $a2z$ and $g1y$ are indeed most important, but the error can be reduced even further by including $a2x$, $a1z$, $a1y$ and $a1x$.

Some input signals could be removed altogether, for example $a2y$ which did not contribute to any output signal.

6. MODEL ESTIMATION AND EVALUATION

To compare the accuracy of different models with respect to accumulated damage, the obvious choice would be to compare the accumulated damage already while creating the models. To do so creates some problems, which are discussed in the following sections.

6.1. ARX model estimation

System identification was used to create models from multiple input signals, to a single output signal. The ARX (AutoRegressive model with eXogenous inputs) structure was chosen for its simplicity. Other models such as ARMAX and Output-Error models were considered, but brief investigations showed that no additional accuracy resulted from using such models. Results from an ARMAX model is compared to an ARX model in Figure 8, and since no major improvement was found, the simpler ARX model was chosen. The typical single input single output ARX-model is given by

Table 2. Signal selection from coherence analysis

Output signal	Good choice of input signals
s1,s2	Steering cylinder pressure.
s3,s4	Steering cylinder pressure & Gyroscope.
s5,s6	Rear accelerometer & gyroscope.
s7,s8	Steering cylinder pressure.
s9	Front accelerometer & Gyroscope.
s10	Rear accelerometer & Gyroscope.
s11,s12	Rear and mid accelerometer.
s13	Steering cylinder pressure & Gyroscope.
s14,s15	Steering cylinder pressure & Gyroscope.
s16	Rear and mid accelerometer.
s17	Rear and mid accelerometer.
s18,s19	No good signal available.

$$y_t + a_1 y_{t-1} + \cdots + a_{n_a} y_{t-n_a} = b_1 u_{t-n_k} + \cdots + b_{n_b} u_{t-n_k-n_b+1} + e_t \quad (5)$$

where y_t is the output at time t and u_t is the input at time t etc. $a_1, \ldots, a_{n_a}$ and $b_1, \ldots, b_{n_b}$ are parameters adjusted to create the best fit of the model.

In matrix notation, expanded to multiple inputs, the expression can be written as a linear regression

$$y(t) = \varphi_t^T \theta + e_t \quad (6)$$

where

$$\begin{cases} \varphi(t) = (-y_{t-1}, \ldots, -y_{t-n_a}, u_t^1, \ldots, u_{t-n_b}^1, u_t^{n_b}, \ldots, u_{t-n_b}^{n_b})^T \\ \theta = (a_1, \ldots, a_{n_a}, b_0^1, \ldots, b_{n_b}^1, b_0^{n_u}, \ldots, b_{n_b}^{n_u}). \end{cases} \quad (7)$$

The multiple input signals are notated with superscripts from 1 to n_u where n_u is the number of input signals. The same notation is used for the corresponding set of parameters $b^1, \ldots, b^{n_u}$

The parameter vector θ in Equation 6 was estimated using a least squares approach. This minimizes the residual between the measured and estimated stress signals, and since the least squares problem is convex, a global optimum is found. Figure 8 show the measured signal together with a simulated output from two models generated. The simulated signal predicts the existence of all peaks and valleys, but underestimates some of the heights and depths. It also shows that only

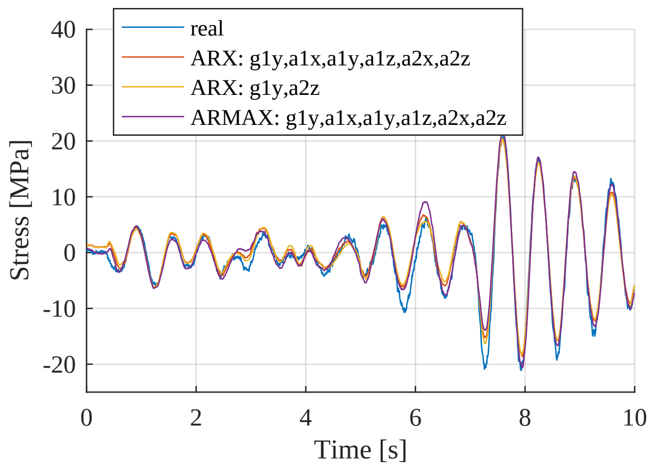

Figure 8. Real and simulated output of s10z, using two different ARX models and one ARMAX model. A two input signal is shown to produce an equally good simulation for this output signal as a model with six input signals. The figure also shows that using the more complex ARMAX model does not considerably improve the result.

two input signals are required to capture most of the signal, as predicted by the investigation in Section 5.3.

6.2. Model bandwidth limitations and effects from noise

The signals investigated showed little or no coherence above 20Hz. The lack of high-frequency coupling resulted in ARX-models unable to capture higher frequency dynamics.

The lack of high-frequency coupling does however not mean that no high frequent components exists in the stress signals, which poses an issue since rain flow counting uses peaks and valleys. The high-frequent oscillations by themselves cause negligible damage, but they cause an underestimation of the large low-frequent cycles, and can have significant effect. This is illustrated in Figure 9. The result is an underestimation of the accumulated damage compared to the measured data as seen in Figure 10.

Yet another issue arises when the accumulated damage is used to evaluate if the model complexity is sufficient. If the model typically underestimates the amplitude of the real stress cycles, this means any erroneous noise caused by the model will falsely seem to improve the model. To compare accumulated damage when evaluating what complexity of model to choose, might therefore be misleading.

The conclusion is, the model is best evaluated by comparing the stress signals directly. This preserves the physical interpretation, and eliminates the risk of a model that relies on noise to create a better fit.

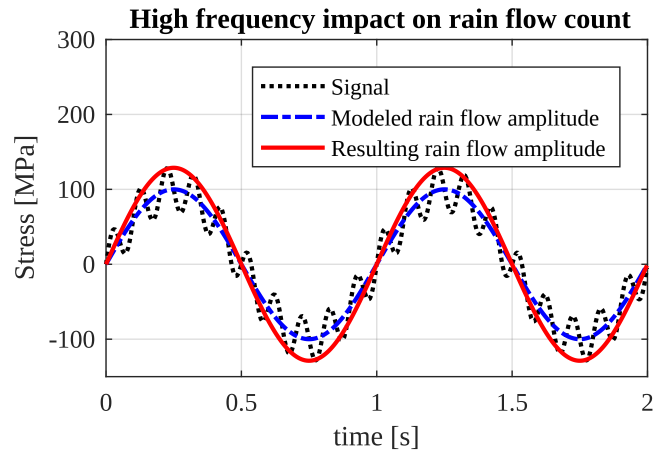

Figure 9. Low pass filtering affects the rain flow count, since the peaks of the main oscillations are superpositioned with the smaller stress oscillations.

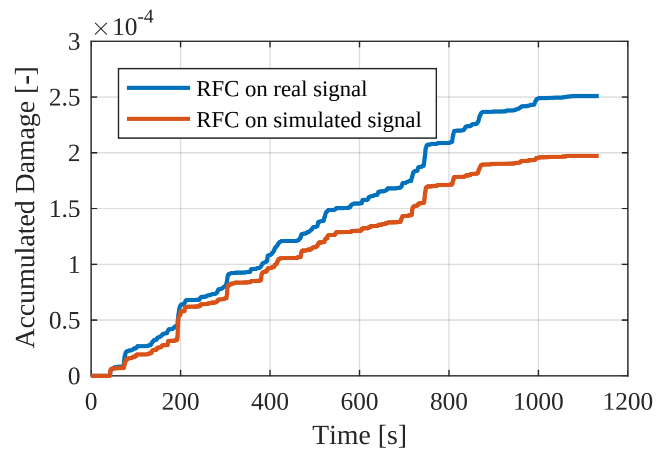

Figure 10. Accumulated damage from measured and simulated signals. Most important cycles are found, which is seen by noticing that fast damage accumulation occurs simultaneously in the real and simulated signal. The total level of damage is underestimated.

7. EFFECTS OF LOAD, ROAD AND SPEED

Several factors has an effect on how fast damage is accumulated. Road conditions and vehicle speeds are directly linked to damage, and can be hard to distinguish from one another. A third important parameter is the mass carried by the vehicle, since it fundamentally changes the dynamics of the model. Ways to handle these parameters are discussed below.

7.1. Dump box load

The amount of load carried by the vehicle has a large impact on the relation between accelerations and stress in the structure. A model identified from data when the truck is loaded, gives highly inaccurate results when the truck is unloaded and vice versa.

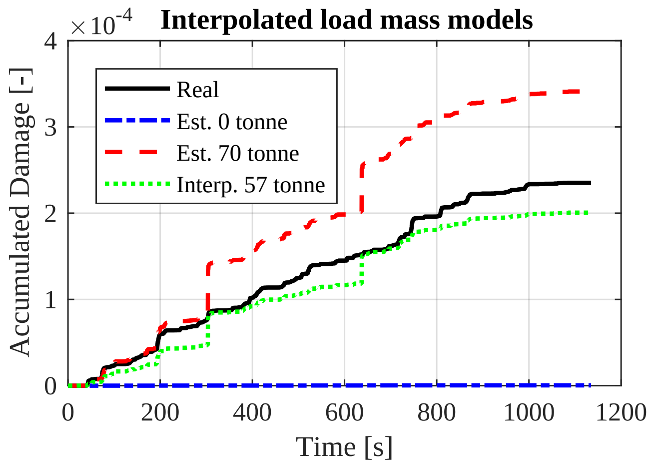

Figure 11. Models created for high and low load levels, are used to generate stress results for a medium load level using interpolation. Accumulated damage from the interpolated stress compares a lot better to the real accumulated damage compared to the individual model outputs.

One way to handle this would be to identify a number of models for different load levels. The stress output from each model can then be interpolated based on load. Two models, 0 tonne and 70 tonne were estimated from corresponding data. Data from the 57 tonne driving case was used as verification data, and compared with the interpolated result from the 0 and 70 tonne models. For this case the interpolated model gave a better approximation of the accumulated damage than either of the other models, as seen in Figure 11.

Due to a lack of data with different load levels, it was hard to verify the linearity of the relationship between load level and structural stress. Gyroscope signals were missing for most of the driving cases with different load levels, and as a result models lacked some accuracy. If additional data was collected, a more reliable interpolation could be performed.

An alternative approach would be to interpolate the accumulated damage directly. Given the non-linear nature of rain flow counting and accumulated damage, a non-linear interpolation method would be required.

7.2. Road conditions

Both road, load, and speed contributes to the accumulated damage of the vehicle. Since the load and speed are measurable, the unknown factor is the condition of the road on which the truck is traveling. For a given speed and load, different road conditions can have a huge impact on the useful life of a machine.

Figure 12 shows the speed while driving multiple laps on a test course. As seen in the zoom section, the speed is almost identical for each lap. This is important when evaluating the roads influence, since higher speed and rougher road conditions can both cause damage, and the relation is not yet fully investigated.

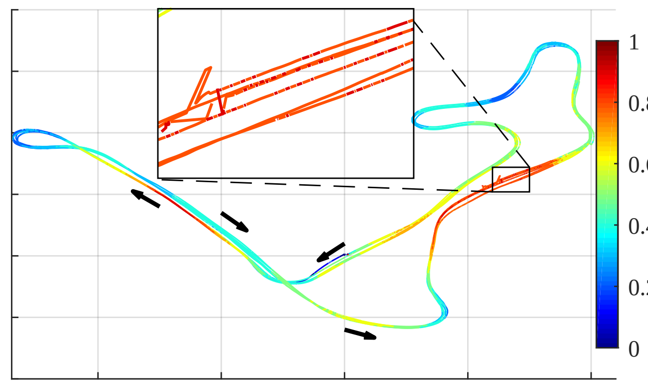

Figure 12. The color of the track shows the speed during the test track drive. Each lap is very similar in speed, making a comparison between track roughness possible.

Figure 13 shows the test track layout, colored by a simulated signal for damage accumulation at location $s10z$. The damage was calculated by performing rain flow count on the stress cycles of $s10z$, and then using Palmgren-Miner's rule to assess the damage from each stress cycle. This resulted in a series of damage instances, each with a corresponding time of occurrence. A moving average filter was applied to allow for better visibility, and the resulting time series was used to visualize the damage in Figure 13.

At the red section around coordinates (150,25), a number of large bumps were placed. During some of the laps, the bumps were used, which is seen in the zoom section of the plot.

Unfortunately, the exact condition of the test track was not recorded during the experiment, and thus no direct connection between surface condition and damage inflicted could be made. Connecting the relative measure to actual surface roughness would be an interesting continuation of this work. To verify the actual performance of the road monitor would require more directed tests with known surfaces. Currently the consistency between laps is the only available performance measure.

When speed is equal for each lap, it is easy to see a difference in road condition. If speed varies, the problem gets more complicated since high damage accumulation rates can either mean rough road, or high speed. Some normalization with respect to speed would be required to get a reliable measure of road condition.

8. LIMITATIONS OF THE MODEL

A large number of parameters effect whether the predicted life from the models in this investigation actually correspond to the actual life of the asset in field. The different limitations can be grouped in two fundamental groups:

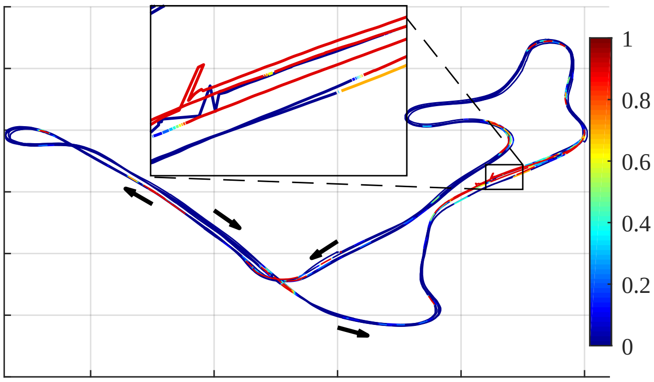

Figure 13. A road roughness measurement consisting of the damage accumulation rate for the simulated stress at $s10z$, plotted along the test track curve. Multiple laps were run, and it can be seen how certain sections consistently cause more damage accumulation than others.

– Limitations verifiable through the stress signal, i.e. factors that result in the stress signal differing from the measured one.
  - Wrong model order
  - Non-linear effects
  - Bad choice of input sensors
  - Lack of coupling between input-output sensors
– External limitations, i.e., even if the stress is perfectly estimated, the actual failure of the asset is not well predicted.
  - Accumulated damage does not correspond to actual failure
  - Stress concentration is more complicated than the assumed constant value.

This work is evaluated with respect to stress and accumulated damage. It is not verified against actual failure of the assets, since such data is unavailable.

9. CONCLUSIONS

A low number of on-board sensors like accelerometers and gyroscopes can give enough information to recreate a stress signal. Together with a linear model, the estimated stress can be accurate enough to evaluate the accumulated fatigue damage in a mining truck.

The linear model structure and the sensors used are unable to capture high frequency behavior. In some cases high frequency cycles are the main drivers for rain flow count and for those cases, the method is likely to be inaccurate.

Combined with known position for the vehicle, it is also possible to draw conclusions about the roads influence for a specific stress location. Both higher speeds and rougher roads cause larger stress amplitudes, and if road conditions and speed are to be separated the proper relationship needs to be investigated.

10. FUTURE WORK

Many steps remain before an online monitoring system is capable of capturing all aspects that drives damage on a mining vehicle. A natural next step is to include external events like loading, unloading and other external forces acting on the vehicle. The accelerometers currently pick up also such signals, but it is not yet verified what model is required to describe the stresses caused by external events.

To create a useful road monitor, one would need to find to evaluate more in detail how speed effects the stress, in relation to how road condition effects the stress.

ACKNOWLEDGMENT

This work was partially supported by the Wallenberg Autonomous Systems and Software Program (WASP)

REFERENCES

ASTM E 1049-85 (Reapproved 1997). (1999). *Standard practices for cycle counting in fatigue analysis* (Vol. Vol. 03.01; Tech. Rep.). Philadelphia.

Byggavdelningen, B., Göransson, L., & Åkerlund, S. (1999). *Boverkets handbok om stålkonstruktioner - bsk 99*. Boverket.

Heine, R., & Barker, D. (2007). Simplified terrain identification and component fatigue damage estimation model for use in a health and usage monitoring system. *Microelectronics Reliability*, *47*(12), 1882 - 1888.

Palmgren, A. (1924). Die lebensdauer von kugellagern. *Zeitschrift des Vereins Deutscher Ingenieure*, *68*(14), 339–341.

Qian, J., Hastie, T., Friedman, J., Tibshirani, R., & Simon, N. (2013). *Glmnet for matlab.* http://www.stanford.edu/~hastie/glmnet_matlab/.

Rupp, A. N. J., Masieri, A., & Dornbusch, T. (2005, 11). Efficient monitoring of loads and stresses under service and test conditions. In *Sae technical paper.* SAE International.

Stephens, R., Fatemi, A., Stephens, R., & Fuchs, H. (2000). *Metal fatigue in engineering*. John Wiley & Sons.

Tibshirani, R. (1996). *Regression shrinkage and selection via the lasso* (Vol. 58) (No. 1).

BIOGRAPHIES

Erik Jakobsson was born in Mjöbäck, Sweden in 1987. He received his M.Sc. in mechanical engineering from Linköping University, Linköping, Sweden, in 2010. After he finished his master's thesis at Atlas Copco Rock Drills AB, he was employed at the rock drill department as a hydraulics design engineer. In 2016 he joined the Wallenberg Autonomous System and Software Program (WASP), and started a new position within Atlas Copco as an industrial PhD student together with Linköping University. His main research interests are related to condition monitoring, sensors in harsh mining environments and the logging and use of on-board sensor data to improve the use and product development of mining machinery.

Erik Frisk was born in Stockholm, Sweden in 1971. He received a PhD degree in 2001 from Linköping University, Sweden. Currently he has a position as an associate professor at the Department of Electrical Engineering at Linköping University. His current research interests in the field of model based diagnosis, prognosis, and autonomous vehicles.

Robert Pettersson was born in Askersund, Sweden in 1981. He received his M.Sc. degree in Vehicle Engineering and Ph.D. degree in Engineering mechanics from the Mechanics department, Royal Institute of Technology, Stockholm, Sweden, in 2006 and 2012, respectively. Since 2012 he is an employee at Atlas Copco Rock Drills as a Specialist in Applied Mechanics. The research interest from the time as Ph.D. student is mechanics and optimization with application to multibody systems. As a professional within mining machinery development, his main interest is in general mechanical analysis and methods for basic development and in his current position he works with e.g. structural analysis (Finite Element Modelling), load measurements and evaluation, analysis of Mechanical Rock Excavation specific topics, stability, and reliability methods.

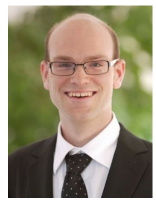

Mattias Krysander was born in Linköping, Sweden in 1977 and is an associate professor at the Department of Electrical Engineering, Linköping University, Sweden. His research interests include model based diagnosis and prognosis and autonomous vehicles. As a way to cope with the complexity and size of industrial systems he has used structural representations of models and developed graph theoretical methods for assisting design of diagnosis systems and for fault isolation and sensor placement analysis. In recent years he has developed data driven techniques for diagnosis and prognosis applications.